International Journal of Power Electronics and Drive System (IJPEDS)
Vol. 8, No. 4, December 2017, pp. 1954~1962
ISSN: 2088-8694, DOI: 10.11591/ijpeds.v8i4.pp1954-1962

A Complete Modeling and Control for Wind Turbine Based of a Doubly Fed Induction Generator using Direct Power Control

Fawzi Senani, Abederrezak Rahab, Hocine Benalla
Laboratoire de l'Electrotechnique de Constantine (LEC), Faculté des Sciences de la Technologie,
Université des frères Mentouri de Constantine 1, Ain el-bey 25000 Constantine, Algerie

Article Info

Article history:

Received Jun 17, 2017
Revised Oct 12, 2017
Accepted Nov 30, 2017

Keyword:

Back-to-back converter
DFIG
DPC
MPPT
WTS

ABSTRACT

The paper presents the complete modeling and control strategy of variable speed wind turbine system (WTS) driven doubly fed induction generators (DFIG). A back-to-back converter is employed for the power conversion exchanged between DFIG and grid. The wind turbine is operated at the maximum power point tracking (MPPT) mode its maximum efficiency. Direct power control (DPC) based on selecting of the appropriate rotor voltage vectors and the errors of the active and reactive power, the control strategy of rotor side converter combines the technique of MPPT and direct power control. In the control system of the grid side converter the direct power control has been used to maintain a constant DC-Link voltage, and the reactive power is set to 0. Simulations results using MATLAB/SIMULINK are presented and discussed on a 1.5MW DFIG wind generation system demonstrate the effectiveness of the proposed control.

Corresponding Author:

Senani Fawzi,
Laboratoire de l'Electrotechnique de Constantine (LEC),
Faculté des Sciences de la Technologie,
Université des frères Mentouri de Constantine 1,
Ain el-bey 25000 Constantine, Algerie.
Email: senani.fouzi@gmail.com

1. INTRODUCTION

Actually, there are several sources of renewable energy, wind energy, hydropower, geothermal energy, biomass, biofuel and solar energy [1]. Wind and solar electric power generation systems are popular renewable energy resources [2]. The wind energy conversion system (WECS) has been considered to be one of the main energy resources are growing rapidly among the other renewable generation power technologies due to its freely available, clean and renewable character [3-5]. Wind energy conversion systems are basically divided into two fixed and variable speed.

Variable speed WECS have been many advantages: operation at maximized power capture over a wide range of wind speeds, reduced mechanical stresses imposed on the turbine, and improved power quality compared with fixed speed WECS[5], [6]. The variable speed WECS using the DFIGs are suitable and promising for application in wind energy. The DFIG is particularly employed for high-power applications, due to the lower converters cost and lower power losses [7].

The WECS based DFIGs control comprises both the rotor side converter (RSC) combines the technique of MPPT and grid side converter (GSC) controllers so that the RSC controls stator active and reactive powers and the GSC regulates dc-link voltage as well as generates an independent reactive power that is injected into the grid [7], [8], for RSC traditionally the vector control (VC) based on a stator flux orientation[7], [9] using proportional–integral (PI) controllers [10], However, it has some disadvantages, such as its dependence on the machine parameters variation, that its performance largely depends on the tuning of the PI parameters, must be optimally tuned to ensure the system stability within the whole operating range

and attain sufficient dynamic response during the transient conditions [7]. In order to overcome the aforementioned problems, different nonlinear control methods such as direct torque control/direct power control (DTC/DPC) have been proposed of DFIG based wind turbine systems has proposed recently [11], [12]. These control methods directly detect the error of torque, flux, active power and reactive power and then choose the desired rotor voltage to IGBTs via a lookup table. The main advantages of DTC/DPC methods include fast response time and less dependence on DFIG parameters, generates the variable-frequency signal. For GSC various control strategies have been proposed. It can be classified for its use of current loop controllers or active/reactive power controllers. The well-known method of indirect active and reactive power control is based on current vector orientation with respect to the line voltage vector. It is called voltage-oriented control (VOC) [13]. However, the final configuration and performance of the VOC system largely depend on the quality of the applied current control strategy. Over the last few years, an interesting emerging control technique has been direct power control (DPC) [14-16]. DPC becomes a study hotspot for its simple control model, there are no internal current loops and no PWM modulator block, fast dynamic response [13], [15], [16], and the converter switching states are appropriately selected by a switching table based on the instantaneous errors, between the, commanded and estimated values of instantaneous active and reactive power, and the power source voltage vector position [14] or virtual-flux vector position [15], [16].

In this study, DFIGs are operated in MPPT mode and, therefore, speed control is necessary and ensured by (IP) regulator for the control strategy on the RSC. This last is controlled by direct power control (DPC) and GSC is controlled by Direct Power Control (DPC).

2. MODELING OF WECS COMPONENTS

A typical WECS configuration has been presented in Figure 1. The considered topology consists of: Turbine via a gearbox connected to DFIGs, which the stator of DFIGs connected directly to the grid and the rotor is connected to back-to-back converter, which includes RSC and GSC [4], [17].

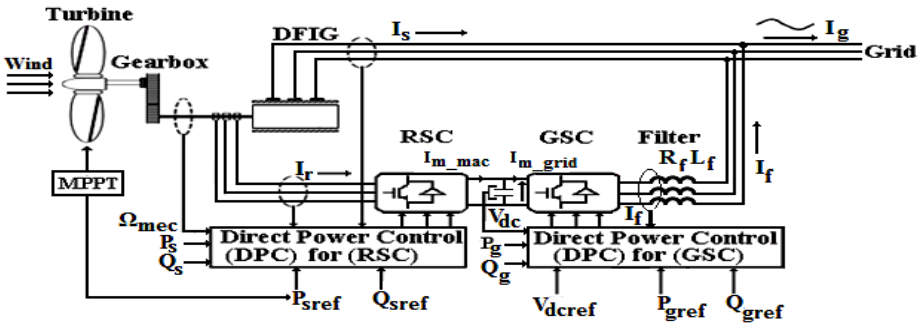

Figure 1. The scheme of variable speed wind turbine system with DFIGs and back-to-back converter system

2.1. Model of Wind Turbine Aerodynamic

The aerodynamic power P_{tur} captured by the wind turbine is given by [17] :

$$P_{tur} = \frac{1}{2}.C_p(\lambda,\beta).\rho.S.v^3 \quad (1)$$

Where: ρ is the air density (1.25 kg/m^3) ; S is wind turbine blades swept area in the wind (m^2) ; R is the turbine radius (m) ; v is wind speed(m/s) ; β blade pitch angle (°) and λ is the tip-speed ratio defined by :

$$\lambda = \frac{\Omega_{tur}.R}{v} \quad (2)$$

C_p is the power coefficient of wind is treated in bibliographies for a wind of 1.5MW [17] , [18]; by:

$$C_p(\lambda,\beta) = \left(0.5 - 0.0167.(\beta-2)\right).sin\left[\frac{\pi.(\lambda+0.1)}{10-0.3.\beta}\right] - 0.00184.(\lambda-3).(\beta-2) \quad (3)$$

Expression of the aerodynamic torque is given by[17]:

$$T_{tur} = \frac{P_{tur}}{\Omega_{tur}} = \frac{\pi}{2.\lambda}\rho.R^3.C_p(\lambda,\beta) \quad (4)$$

The gearbox is the connection between the turbine and the generator modeled by [17] :

$$T_{mec} = \frac{T_{tur}}{G} \quad (5)$$

$$\Omega_{mec} = G.\Omega_{tur} \quad (6)$$

Where: T_{mec} is mechanical torque, Ω_{tur}, Ω_{mec} are the turbine and generator speed, and G is the gearbox ratio.
The equation of system dynamics, can be written as [17]

$$J\frac{d\Omega_{mec}}{dt} + f.\Omega_{mec} = T_{mec} - T_{em} \quad (7)$$

Where: f is the viscous friction coefficient, T_{em} is the electromagnetic torque of the generator.

2.2. Model of Doubly Fed Induction Generator

The electrical equations of the stator and rotor voltages of the DFIG are written[17], [18]:

$$\begin{cases} V_{sd} = R_s I_{sd} + \frac{d\varphi_{sd}}{dt} - \omega_s \varphi_{sq} \\ V_{sq} = R_s I_{sq} + \frac{d\varphi_{sq}}{dt} + \omega_s \varphi_{sd} \\ V_{rd} = R_r I_{rd} + \frac{d\varphi_{rd}}{dt} - \omega_r \varphi_{rq} \\ V_{rq} = R_r I_{rq} + \frac{d\varphi_{rq}}{dt} + \omega_r \varphi_{rd} \end{cases} \quad (8)$$

The stator and rotor flux are expressed by [17], [18]:

$$\begin{cases} \varphi_{sd} = L_s I_{sd} + M I_{rd} \\ \varphi_{sq} = L_s I_{sq} + M I_{rq} \\ \varphi_{rd} = L_r I_{rd} + M I_{sd} \\ \varphi_{rq} = L_s I_{rq} + M I_{rq} \end{cases} \quad (9)$$

Where: R_s, R_r, L_s and L_r are respectively the resistance and inductance of the stator and the rotor ; M is the mutual inductance, I_{sd}, I_{sq}, I_{rd}, I_{rq} represent the d and q components of the stator and rotor currents ; ω_s is the statar angular frequency ($\omega_r = \omega_s - P.\Omega_{mec}$); $\omega_{r\,is}$ rotor angular frequency.and P number of pole pairs.
Equation (10) represents the expression of electromagnetic torque [17] :

$$T_{em} = p\frac{M}{L_s}\left(\varphi_{sd} I_{rq} - \varphi_{sq} I_{rd}\right) \quad (10)$$

2.3. Modeling of the Connection of Grid Side Converter

The capacitor current and The voltage across the capacitor of DC-Link voltage are obtained [19] :

$$\begin{cases} I_c = I_{m\_grid} - I_{m\_mac} \\ \frac{dV_{dc}}{dt} = \frac{1}{C}.I_c \end{cases} \quad (11)$$

Elsewhere, the grid phase voltages can be expressed [19] :

$$\begin{cases} V_{ga} = R_f I_{fa} + L_f \frac{dI_{fa}}{dt} + V_{fa} \\ V_{gb} = R_f I_{fb} + L_f \frac{dI_{fb}}{dt} + V_{fb} \\ V_{gc} = R_f I_{fc} + L_f \frac{dI_{fc}}{dt} + V_{fc} \end{cases} \quad (12)$$

Where: I_{m_mac}, I_{m_grid} are the currents modulated by the RSC and the GSC; R_f, L_f : resistance and inductance of the grid filter ; V_{fa}, V_{fb}, V_{fc} : inputs voltages of the GSC ;I_{fa}, I_{fb}, I_{fc} : The currents flowing through the filter.

3. CONTROL STRATEGIES OF WECS

The control strategy used in this paper includes the MPPT algorithm by controlling speed of DFIG, the DPC for RSC by controlling the stator active and reactive powers and the DPC for GSC by controlling the DC-Link voltage and active and reactive powers exchanged with grid.

3.1. Maximum Power Point Tracking with Speed Control

For this study, it will be assumed, whatever the power generated, the electromagnetic torque developed is at all times equal to its reference value T_{em}=T_{emref} [17], [18].

This technique consist of determining the speed of the turbine Ω_{tur} which makes it possible to obtain the maximum power generated. Thus, the electromagnetic torque must be adjusted on the DFIG shaft so as to fix the rotational speed of at a reference speed at the output of the speed controller (I-P) [17] (Figure 2).

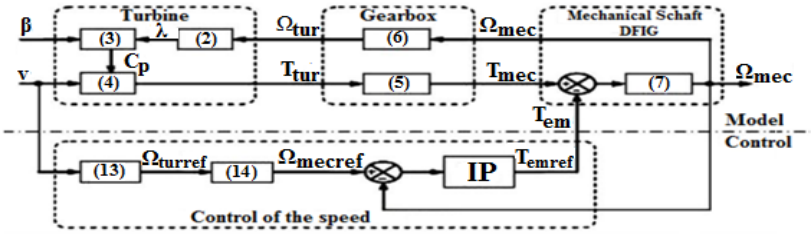

Figure 2. Model of Turbine with speed control of the generator

The Ω_{turref} corresponds to that of the optimum value of the λ_{opt} allowing it possible to obtain the maximum value of the Cpmax we can write:

$$= \frac{\lambda_{opt}.v}{R} \quad (13)$$

This reference speed depends on the Ω_{turref} to be fixed to maximize the extracted power, we have:

$$\Omega_{mecref} = G.\Omega_{turbref} \quad (14)$$

3.2. Direct Power Control of DFIG with Rotor Side Converter

DPC was originally developed for the PWM control of power inverters [15], [16]. Eventually, given its fast, yet robust and precise power tracking capabilities, DPC has become one of the main control strategies for DFIG-based WECS [11]. It is based in which the controls of active and reactive powers are directly controlled, without the intermediate step of using current regulators as in field oriented control. In fact, it is based on the determination of instantaneous rotor vectors in each sampling period regarding desired stator active and reactive powers.

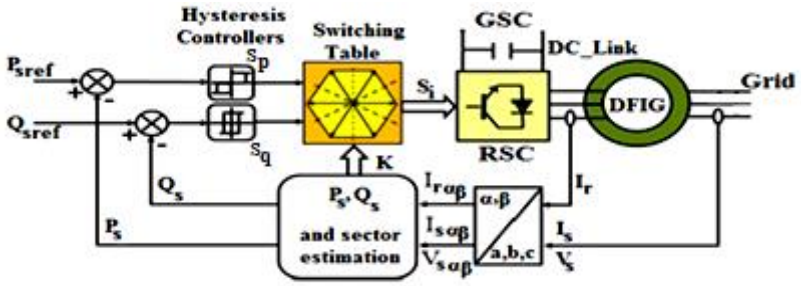

Figure 3. Basic DPC bloc diagram

The block diagram of the conventional DPC is depicted in Figure 3. As it is shown, the computed values of stator active and reactive powers are compared to the corresponding references, and the errors are sent to 3-level and 2-level hysteresis regulator proposed for active power controller and reactive power controller respectively [11]. Using the outputs of hysteresis comparators and also the sector number which stator flux in rotor frame lies in, a proper voltage vector is selected from the switching table [11].

If stator and rotor resistances are neglected indicate that, having a constant stator flux φ_s and the rotor flux is obtained from equation(15), it is indicate that variation of rotor flux is dependent to applied rotor voltage [5], [20].

$$\frac{d\varphi_r^r}{dt} = V_r^r - R_r I_r^r \approx V_r^r \tag{15}$$

Where: $\varphi_r{}^r$, $V_r{}^r$ and $I_r{}^r$ are the rotor flux, voltage and current, expressed in the frame linked to the rotor.

Therefore, by selecting an appropriate voltage vector, $\varphi_r{}^r$ can be controlled. Thus, if the position of stator flux in rotor frame is known, the change of $\varphi_r{}^r \sin\delta$ and $\varphi_r{}^r \cos\delta$ is achieved.

Where: δ the angle between stator and rotor flux vectors.

The eight voltage vectors of a two-level RSC which the vector plane is divided to six sectors

Instantaneous active and reactive powers can be estimated from relationships [12]:

$$\begin{cases} P_s = \frac{3}{2}\left(V_{s\alpha} I_{s\alpha} + V_{s\beta} I_{s\beta}\right) \\ Q_s = \frac{3}{2}\left(V_{s\beta} I_{s\alpha} - V_{s\alpha} I_{s\beta}\right) \end{cases} \tag{16}$$

The digitized error signal Sp and Sq and the rotor flux sector are input to the switching table in which every switching state S_a, S_b and S_c of the converter as shown in Table 1[20].

Table 1 Optimal switching table for RSC

S_q	S_p	δ_1	δ_2	δ_3	δ_4	δ_5	δ_6
	1	V_2	V_3	V_4	V_5	V_6	V_1
0	0	V_0	V_7	V_0	V_7	V_0	V_7
	1-	V_6	V_1	V_2	V_3	V_4	V_5
	1	V_3	V_4	V_5	V_6	V_1	V_2
1	0	V_7	V_0	V_7	V_0	V_7	V_0
	1-	V_5	V_6	V_1	V_2	V_3	V_4

3.3. Direct Power Control of Grid Side Converter

The main idea of DPC is similar to the well-known direct torque control (DTC) for induction motors. Instead of controlling torque and flux, the instantaneous active Pg and reactive Qg powers are controlled [14-16]. The block scheme of DPC for GSC is shown in Figure 4.

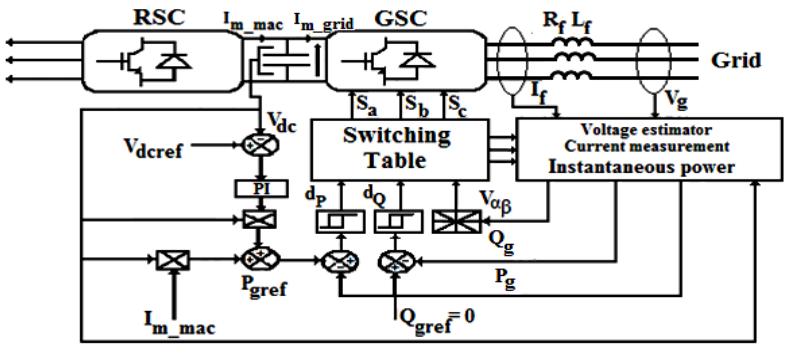

Figure 4. Direct power control for GSC

The main idea of voltage based power estimation for DPC was proposed in [14]. The instantaneous values of active and reactive powers in grid voltage sensorless system are estimated by:

$$\begin{cases} P_g = L_f\left(\frac{dI_{ga}}{dt}I_{ga} + \frac{dI_{gb}}{dt}I_{gb} + \frac{dI_{gc}}{dt}I_{gc}\right) + V_{dc}\left(S_aI_{ga} + S_bI_{gb} + S_cI_{gc}\right) \\ Q_g = \frac{1}{\sqrt{3}}\left[3L_f\left(\frac{dI_{ga}}{dt}I_{gc} + \frac{dI_{gc}}{dt}I_{ga}\right) - V_{dc}\{S_a(I_{gb} - I_{gc}) + S_b(I_{gc} - I_{ga}) + S_c(I_{gc} - I_{ga})\}\right] \end{cases} \quad (17)$$

The grid-line voltage sector is necessary to read the switching table; therefore knowledge of the line voltage is essential. However, once the estimated values of active and reactive power are calculated and the grid-line currents are known, the line voltage can easily be calculated as [13], [14].

$$\begin{bmatrix} V_{g\alpha} \\ V_{g\beta} \end{bmatrix} = \frac{1}{I_{f\alpha}^2 + I_{f\beta}^2}\begin{bmatrix} I_{f\alpha} & -I_{f\beta} \\ I_{f\beta} & I_{f\alpha} \end{bmatrix}\begin{bmatrix} P_g \\ Q_g \end{bmatrix} \quad (18)$$

The commands of reactive power Q_{gref} set to zero for unity power factor and active power P_{gref} is obtained after being added to the P_{cref} delivered from the outer PI-DC-Link voltage controller the power generated by the DFIG $P_{m\_mac} = I_{m\_mac}.V_{dc}$ are compared with the estimated Q_g and P_g values, in reactive and active power two-level hysteresis controllers, respectively [4].

The digitized variables d_p,d_q and the line voltage vector position $\theta = \tan^{-1}(V_{g\alpha}/V_{g\beta})$ form a digital word, which by accessing the address of lookup table selects the appropriate voltage vector according to the switching table[16], [21]. For this purpose, the stationary coordinates are divided into 12 sectors [21] :

Table 2 shows the switching table for GSC

Table 2 Switching table for GSC

d_P	d_Q	θ_1	θ_2	θ_3	θ_4	θ_5	θ_6	θ_7	θ_8	θ_9	θ_{10}	θ_{11}	θ_{12}
1	0	V_6	V_7	V_1	V_0	V_2	V_7	V_3	V_0	V_4	V_7	V_5	V_0
	1	V_7	V_7	V_0	V_0	V_7	V_7	V_0	V_0	V_7	V_7	V_0	V_0
0	0	V_6	V_1	V_1	V_2	V_2	V_3	V_3	V_5	V_4	V_6	V_6	V_1
	1	V_1	V_2	V_2	V_3	V_3	V_4	V_4	V_5	V_4	V_6	V_6	V_1

4. SIMULATION RESULTS AND ANALYSIS

The simulation of the wind system based on a DFIG with the considered control systems illustrated in Figure 1 has been implemented in MATLAB/Simulink. The parameters used are given in the annexes.

Figure 5 shows the example of wind profile applied to the studied system; two speed wind profile equal to 11 m/s (0s to 5s) and 18 m/s (5s to 10s) which corresponds to two operating points one in hypo synchronous mode and the other in hyper synchronous mode.

Figure 6 shows the waveforms of optimal reference speed and measured speed of DIFG obtained from simulation of control system. It can be seen, that the generator speed is accurately adjusted to the waveforms of optimal reference speed, which is obtained from MPPT.

Figure 7 and Figure 8 shows the DFIG stator active and reactive powers with their references. The stator active power reference is obtained by the MPPT control. The reference of reactive power maintained at zero to ensure a unit power factor in order to optimize the quality of the energy returned to the grid. DPC for DFIG see a good performances and the robustness of the power control compared with vector control.

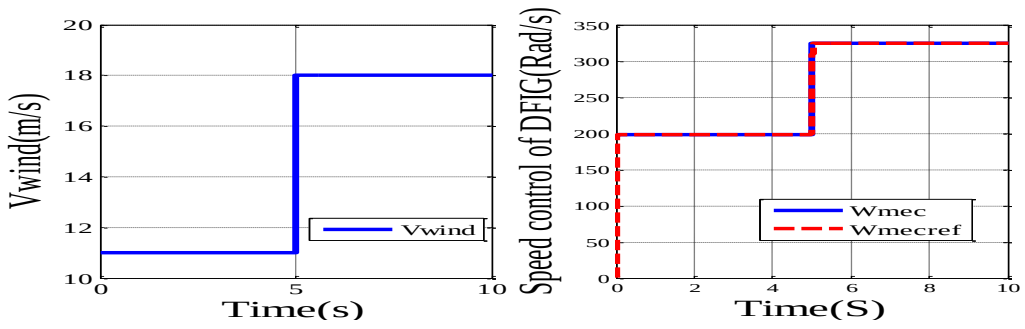

Figure 5. Wind speed profile

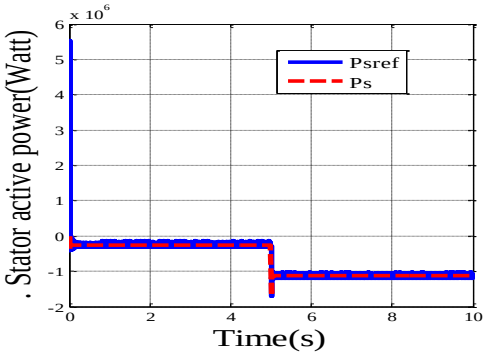

Figure 6. Speed control of DFIG

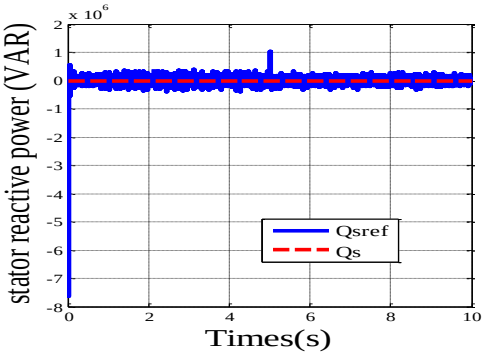

Figure 7. Stator active power control

Figure 8. Stator reactive power control

The Figure 9 presents the waveform of the DC link voltage; The DC link voltage reference is set to 1200 V, the measured voltage perfectly follows the reference voltage with the exception of the initial conditions where the voltage control loop does not have enough time to react, at 5s light variation of DC-Link voltage due to the passage of hypo synchronous mode to the hyper synchronous mode.

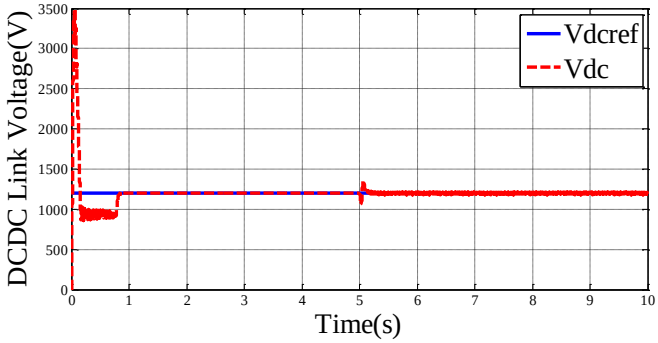

Figure 9. DC Link Voltage control

Figure 10 and 11 shows the instantaneous active and reactive power delivered to the grid follows their references. From Figure 11, it can be noticed, that the instantaneous reactive power is constantly maintaining at zero values, while the active power changes at 5s of a value positive to a value negative.

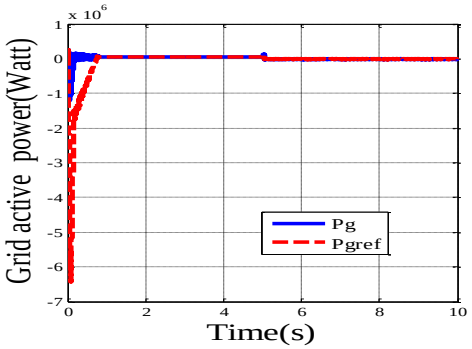

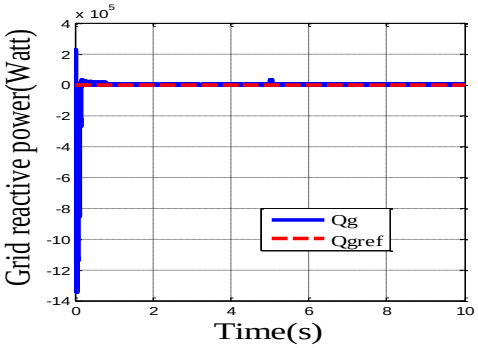

Figure 10. Grid active power control

Figure 11. Grid reactive power control

Figure 12 presents the waveforms of the grid phase voltage and filter phase current. during (t=1s to 5s), are in phase directly, the DFIG rotor absorbs active power from the grid (hypo-synchronous), and (t = 5s to 10s) are in antiphase, so the DFIG rotor also provides active power to the grid (hyper-synchronous).

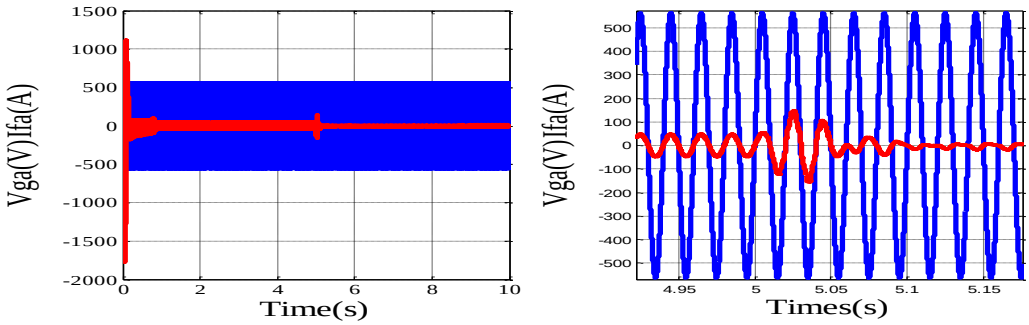

Figure 12. Grid voltage and filter current

5. CONCLUSION

In this paper the dynamic modeling and control of wind energy conversion system with variable speed driven DFIG is presented with a wind profile a two operating points: hypo and hyper synchronous. The control of DFIG with RSC is based in direct power control with cooperation of MPPT algorithm including speed generator control based on IP controller, the DPC of generator is capable of decoupled control of stator active and reactive power without rotor position sensors and has been in an optimal power controller for maximum energy capture in wind energy application, DPC show the faster time reponce. DPC of GSC enables to keep the DC-Link voltage to reference value based on the PI controller and to adjust the reactive power of the system. The DPC not using internal current control loops and no PWM modulator block. By analyzing it is determined that the DPC provides a good dynamic of the system and keeps its robustness.

The simulation results of WECS obtained are satisfactory, have a good performance and good control proprieties between measured and reference quantities (speed generator, stator and grid active and reactive power, DC-Link voltage). The combined VC and DPC (VCDPC) in WECS are very promising.

ANNEXES

Parameters of Turbine [18]
Rated Power of Turbine=1.5MW; R=35.25m; G=90.
Parameters of DFIG [18]
Rated Power of DFIG=1.5MW; V_s=690V; R_s=0.012Ω; R_r=0.021Ω; L_s=0.0137H; L_r=0.0136H; M=0.0135H; J=1000kg.m^2; f=0.0024kg.m^2/s; P=2.
Parameters of Filter R_fL_f and Capacitor of DC-Link voltage [18]
R_f=2.10^{-3} Ω; L_f=2.10^{-3}H; C=4400µF.

REFERENCES

[1] Dahech K., Allouche M, Damak T, Tadeo F, "Backstepping sliding mode control for maximum power point tracking of a photovoltaic system," *Electric Power Systems Research*. 2017; 143:182–188.
[2] Ananth D.V.N, Kumar G.V.N., "Flux Based Sensorless Speed Sensing and Real and Reactive Power Flow Control with Look-up Table based Maximum Power Point Tracking Technique for Grid Connected Doubly Fed Induction Generator," *Indonesian Journal of Electrical Engineering and Informatics (IJEEI).* December 2015; 3(4): 239-260.
[3] Rahab A, Senani F, Benalla H., "Direct Power Control of Brushless Doubly-Fed Induction Generator Used in Wind Energy Conversion System," *International Journal of Power Electronics and Drive System (IJPEDS)*. March 2017; 8(1): 417-433.
[4] Ghennam T, Aliouane K, Akel F, Francois B, Berkouk E.M., "Advanced control system of DFIG based wind generators for reactive power production and integration in a wind farm dispatching," *Energy Conversion and Management*. 2015; 105: 240–250.
[5] Yousefi-Talouki A, Pouresmaeil E, Jorgensen B.N., "Active and reactive power ripple minimization in direct power control of matrix converter-fed DFIG," *Electrical Power and Energy Systems*. 2014; 63: 600–608.
[6] Mohammadi J, Vaez-Zadeh S, Afsharnia S, Daryabeigi E., "A combined vector and direct power control for DFIG-based wind turbines," *In: IEEE Trans Sustain Energy.* 2014; 29(3): 767–75.
[7] Mohseni M, Islam S, Masoum M. A. S., "Enhanced hysteresis-based current regulators in vector control of DFIG wind turbines," *IEEE Trans. Power Electron*. Jan. 2011; 26(1): 223–234.

[8] Zerzouri N, Labar H., "Active and Reactive Power Control of a Doubly Fed Induction Generator," *International Journal of Power Electronics and Drive System (IJPEDS)*. October 2014; 5(2): 244-251.
[9] Boulahia A, M Adel, Benalla H., "Predictive Power Control of Grid and Rotor Side Converters in Doubly Fed Induction Generators Based Wind Turbine," *Bulletin of Electrical Engineering and Informatics*. December 2013; 2(4): 258-264.
[10] Muller S, Deicke M, De Doncker R.W., "Doubly fed induction generator systems for wind turbines," *IEEE Ind. Appl. Mag*. 2002; 8(3): 26–33.
[11] Xu L, and Cartwright P., "Direct active and reactive power control of DFIG for wind energy generation," *IEEE Trans. Energy Convers*. Sep. 2006; 21(3) :750–758.
[12] Hu J, Nian H, Hu B, He Y., "Direct active and reactive power regulation of DFIG using sliding-mode control approach," *IEEE Trans. Energy Convers*. Dec. 2010; 25(4): 1028–1039.
[13] Malinowski M, Kazmierkowski M.P, Trzynadlowski A., "Review and comparative study of control techniques for three-phase PWM rectifiers," *Mathematics and Computers in Simulation*. 2003; 63: 349–361.
[14] Noguchi T, Tomiki H, Kondo S, Takahashi I., "Direct power control of PWM converter without power-source voltage sensors," *IEEE Trans Ind Appl.* 1998; 34: 941–946.
[15] Malinowski M, Kazmierkowski M.P, Hansen S, Blaabjerg F, Maeques G.D., "Virtual flux based direct power control of three phase PWM rectifiers," *IEEE Trans Ind Appl*. 2001; 37(4): 1019–1027.
[16] Malinowski M, Jasinski M, Kazmierkowski M.P., "Simple direct power control of three phase PWM rectifier using space vector modulation (DPC–SVM)," *IEEE Trans Ind Electron*. 2004; 51(2): 447–454,.
[17] Gaillard A., "Wind system based on the DFIG: contribution to the study of the quality of the electric energy and the continuity of service," *Phd Thesis, Henri Poincare University, Nancy-I, France*; April 2010.
[18] El Aimani S., "Modeling of Various Integrated Wind Turbine Technologies in a Medium Voltage Grid," *PhD Thesis, Ecole Centrale de Lille*, 2004.
[19] Xu L., "Coordinated control of DFIG's rotor and grid side converters during network unbalance," *IEEE Transactions on Power Electronics*. 2008; 23: 1041-1049.
[20] Tremblay E, Atayde S, Chandra A., "*Direct power control of a DFIG-based WECS with active filter capabilities*," in Electrical Power & Energy Conference, EPEC 2009. IEEE, 2009: 1-6.
[21] Chaoui A, Krim F, Gaubert J, Rambault L., "DPC controlled three-phase active filter for power quality improvement," *Electr Power Energy Syst. 2008;* 30: 476–485.